



Published in final edited form as:

Nat Plants. ; 2: 16110. doi:10.1038/nplants.2016.110.

Genetic architecture and pleiotropy shape costs of *Rps2*-mediated resistance in *Arabidopsis thaliana*

Alice MacQueen^{1,2}, Xiaoqin Sun^{1,3}, and Joy Bergelson^{1,*}

¹ Department of Ecology and Evolution, University of Chicago, 1101 East 57th Street, Chicago, IL 60637, USA.

Abstract

The mounting evidence that *R*-genes incur large fitness costs raises a question: how can there be a 5-10% fitness reduction for all 149 *R*-genes in the *Arabidopsis thaliana* genome? The *R*-genes tested to date segregate for insertion-deletion (indel) polymorphisms where susceptible alleles are complete deletions. Since costs of resistance are measured as the differential fitness of isolines carrying resistant and susceptible alleles, indels reveal costs that may be masked when susceptible alleles are expressed. *Rps2* segregates for two expressed clades of alleles, one resistant and one susceptible. Plants with resistant *Rps2* are not less fit than those with a susceptible *Rps2* allele in the absence of disease. Instead, all alleles provide a fitness benefit relative to an artificial deletion, due to the role of RPS2 as a negative regulator of defense. Our results highlight the interplay between genomic architecture and the magnitude of costs of resistance.

Understanding how plants maximize fitness in response to intermittent pathogen presence is of central importance in plant pathology. Natural plant pathosystems frequently involve long-maintained polymorphisms for host resistance¹⁻³, and current theory on the maintenance of stable resistance polymorphisms requires costs of resistance and/or virulence acting in combination with frequency dependent selection⁴. In contrast, in agricultural contexts, resistance genes often have useful lifespans of only a few years and high costs of resistance are undesirable due to their negative effects on plant performance⁵. Pathogen resistance may involve two distinct fitness costs. The first, which we term a cost of surveillance, accrues from harboring *R*-genes that allow a resistance response upon attack⁶, and the second, a cost of defense, accrues from activation of the resistance response during attack^{6,7}.

Users may view, print, copy, and download text and data-mine the content in such documents, for the purposes of academic research, subject always to the full Conditions of use:http://www.nature.com/authors/editorial_policies/license.html#terms

*To whom correspondence should be addressed. jbergels@uchicago.edu.

²current address: Department of Integrative Biology, University of Texas at Austin, 1 University Station #C0930, Austin, TX 78712, USA.

³current address: Institute of Botany, Jiangsu Province and Chinese Academy of Sciences, Nanjing 210014, China.

Author Contributions

XQS created the allelic series; AM, XQS, and JB designed the experiments; AM conducted the experiments, JB conceived of the experiments, AM and JB wrote the paper.

The authors declare they have no competing financial interests.

A cost of surveillance is measured in the absence of disease and has been determined for two *R*-genes, *Rps5* and *Rpm1*, in *Arabidopsis thaliana*^{8,9}. *Rps5* exists in nature as a long-lived insertion-deletion polymorphism (indel) for resistance (*R*) and susceptibility (*S*)^{1,10,11}; *Rpm1* similarly exists as a long-lived indel polymorphism, though secondarily disrupted *S* alleles are also present within the resistance clade¹². In both cases, resistant isolines suffer a 5-10% fitness cost relative to null isolines^{8,9}. However, costs of this magnitude would correspond to an impossibly high genetic load if seen for all, or many, of the ~149 *R*-genes in *A. thaliana*. We propose that indels are an architecture with unusually high costs of surveillance. Null alleles of indels cannot carry any burden of mis-expression or mis-activation that would reduce relative costs of carrying resistant versus susceptible alleles. Furthermore, null alleles do not have the potential to evolve pleiotropic or alternative functions, another means of ameliorating costs of surveillance. *R*-genes are found with a great diversity of genetic architectures, including single loci with many, functional alleles and arrays of tandem duplicated *R*-genes¹³. Here, we explore the possibility that *R*-gene genetic architectures with alternative functional alleles have substantially smaller costs than those of the indels *Rpm1* and *Rps5*. We posit that the large costs associated with these two *R*-genes are precisely the reason susceptible alleles are deleted.

Rps2 exists as an ancient balanced polymorphism with two long-lived clades of alleles, one resistant and one susceptible to *Pseudomonas syringae* pv. *avrRpt2*^{14,15}. Both clades are maintained at intermediate frequencies in local populations¹⁶. *Rps2* is also present in every accession sequenced to date¹⁷. To measure the surveillance cost associated with resistant alleles of *Rps2*, we assayed fitness in the absence of disease for a transgenically-created allelic series of *Rps2* that controls for the insertion site of the *R*-gene alleles¹⁸. We extended the basic strategy of using a Cre-lox system to compare isolines with and without a resistant allele (as done for *Rpm1*⁸ and *Rps5*⁹) to precisely integrate five alleles of *Rps2* into the same genomic location. These alleles were inserted into a Col-0 genetic background in which *Rps2* had been knocked out¹⁵. We additionally verified the robustness of our results by using three genomic locations for the insertion of *Rps2*. Our results reveal a bidirectional interplay between genomic architecture and fitness costs of resistance.

Results

No cost of surveillance for *R* alleles relative to *S* alleles of *Rps2*

To test for surveillance costs of *Rps2* alleles, we measured the lifetime fitness of three resistant (*Rps2^R*) and one partially resistant (*Rps2^{pR}*) isolines relative to one susceptible (*Rps2^S*) allele at each of three genomic insertion sites in a field experiment performed in the absence of pathogens carrying *avrRpt2* (Figure 1, Supplementary Figure 1 and Supplementary Table 1). After correction for multiple testing, there were no significant differences in the fitness proxies of isogenic plants carrying *Rps2^{pR}* and *Rps2^S* alleles at the same insertion site (Supplementary Tables 2-4). Significant differences in correlations between fitness proxies might reveal differential resource allocation across resistance classes; however, such differences in fitness proxy correlations were not evident between *Rps2^R*, *Rps2^S*, and *Rps2^{pR}* lines after a multiple testing correction (Fisher's *z* test, NS). Two fitness proxies supported higher, rather than lower, fitness for *Rps2^R* alleles than *Rps2^S*

alleles (Supplementary Table 3). At the anti-conservative 5% level, there was no consistency in the fitness benefit of susceptible, resistant or partially resistant alleles when integrated into the same genomic location (Supplementary Tables 2-4). Additionally, there was considerable variation in the fitness associated with particular susceptible or resistant alleles across insertion sites (Figure 2a-c).

Expression levels can alter the penetrance of phenotypes¹⁹, and overexpression of *Rps2* can lead to nonspecific activation of the hypersensitive response (HR), or even lethality, if expression levels are too high^{20,21}. The expression of each allele varied within and across insertion sites when transgenic plants were measured in growth chamber conditions (Supplementary Figure 2), and in many cases *Rps2* expression was two- to four-fold higher in the isolines than in the accessions from which the alleles derived (Supplementary Figure 3). To investigate the relationship between fitness variation and *Rps2* expression, we modeled lifetime seed production in the field as a linear function of average *Rps2* expression at 23 days for each allele nested within allele class (Figure 2f; Supplementary Table 5). We also included as a covariate the date at which each plant was collected from the field. For both the *Rps2^R* and *Rps2^S* classes, basal expression of *Rps2* was negatively correlated with lifetime fitness (Figure 2f; $F = 9.666$; $df = 8, 602$; $R^2 = 0.114$, p values = 0.0028, 0.024), although the negative correlation for the *Rps2^P* class was not significant (p value = 0.73). These results indicate that *Rps2* overexpression is costly in the absence of pathogens for both *R* and *S* clade alleles. Adding *Rps2* expression into the fitness model did not reveal differences in performance that were masked by differences in expression between *Rps2^R*, *Rps2^P*, and *Rps2^S* lines (Supplementary Table 5).

An artificial *Rps2* knockout is significantly less fit in the absence of pathogens

If resistant and susceptible alleles have equivalent fitness in the absence of pathogens, then the benefit of *Rps2^R* resistance should have driven the *Rps2^R* clade to fixation. However, both clades have been maintained for millions of years in *A. thaliana*¹⁶. We hypothesized that *Rps2^S*, and perhaps *Rps2^R*, alleles must have another beneficial function to permit maintenance of the *Rps2^S* clade. To explore this possibility, we compared the fitness of all lines with an expressed allele of *Rps2* (collectively, *Rps2⁺*) to three artificial knockout isolines (*Rps2^{KO}*), using the same field experiment performed in the absence of pathogens carrying *avrRpt2*. In 19 out of 21 comparisons using seven fitness proxies for alleles at each of the three insertion sites, *Rps2⁺* isolines demonstrated higher performance than *Rps2^{KO}* isolines, although after correction for multiple testing, only five of these instances were significant (Supplementary Tables 6-8). In terms of lifetime seed set, *Rps2^{KO}* individuals suffered up to a 54% reduction relative to *Rps2⁺* isolines (Figure 2a-c); this fitness cost was significant for the five lines with the lowest *Rps2* expression. This pattern follows from the negative correlation between basal *Rps2* expression and lifetime fitness in both *Rps2^R* and *Rps2^S* allele classes (Figure 2f), such that highly expressing *A. thaliana* lines suffered a fitness reduction much like that observed in the knockout lines. Interestingly, the comparisons revealing a significant cost of the *Rps2* knockout include *Rps2⁺* lines with expression levels most similar to native accessions (Supplemental Figure 3; Figure 2f). *Rps2^{KO}* individuals also had a significantly weaker correlation between plant weight and total collected seed (Fisher's z test $p = 4.8E-06$) than plants with any other allele of *Rps2*

(correlation coefficient of 0.85 compared to all > 0.93); this pattern was driven by a number of *Rps2*^{KO} plants with much lower seed sets than expected for their weight. Taken together, these results suggest that low expression of any allele of *Rps2* is beneficial in the absence of known *Rps2*-mediated pathogens carrying *avrRpt2*.

We considered two hypotheses to explain the observed benefit of all *Rps2* alleles in the absence of *P. syringae* pv. *avrRpt2*. First, the presence of a different, and undetected, pathogen recognized by all alleles of *Rps2* in the field may have provided a benefit to isolines carrying alleles susceptible to *avrRpt2*. Alternatively, a pleiotropic function for *Rps2* in the absence of disease may have contributed to its benefit. To discriminate between these hypotheses, we first repeated our fitness experiment in a growth chamber that mimicked the stressful environmental conditions of our field environment but was known to be free of RPS2-recognized pathogens. Due to size constraints of the growth chamber, we used isolines from only one insertion site in this experiment. As in the field experiment, after correction for multiple testing, there were no significant differences in fitness proxies between *Rps2*^R or *Rps2*^{PR} lines relative to *Rps2*^S lines (Figure 2d; Supplementary Table 9; F = 9.20, df = 9, 1009, *p* value > 0.003). Again, *Rps2*⁺ lines set significantly more seed than *Rps2*^{KO} lines (Supplementary Table 10; F = 39.8, df = 2, 875, *p* value = 0.006). Thus, the growth chamber results recapitulated the results seen in the field.

As a final confirmation that the observed fitness difference was not due to an interaction with an unknown microbe, we grew our isolines from one insertion site in sterile conditions on agar. Again, *Rps2*⁺ plants had a higher weight than *Rps2*^{KO} plants at 21 days (Figure 2e, F = 9.63, df = 1, 114, *p* value = 0.0024). This result excluded the possibility that the presence of *Rps2* carried a fitness benefit due to recognition of pathogens.

Our isolines were all created using a Cre-lox system in the *rps2-101C* mutant background. It should be noted that, though this background is often used as an *Rps2* null^{7,20-27}, it nonetheless produces a 235 amino acid, N' terminal fragment of an RPS2 protein which contains the entirety of the RPS2 coiled-coil domain. In addition, our constructs could have anti-sense transcription of RPS2, as is seen for the native copy of RPS2, or ectopic expression of the last three exons of *At4g26100*. Though previous work has demonstrated that truncation mutants of RPS2 are not autoactive^{21,28} and do not interact with typical RPS2-interacting proteins²¹, we sought to test that this truncated *RPS2-101c* protein, anti-sense transcript and/or the presence of nptII and lox sites did not contribute to plant performance. To do this, we compared the fitness of a transgenic *Rps2*^{KO} line, created in the *rps2-101C* background and containing lox sites at insertion site two, with an independently created Col-0 amiRNA knockdown of *Rps2* grown under sterile conditions (Supplementary Figure 4). There were no significant differences in weight between these two susceptible lines (*p* value > 0.65). We additionally failed to detect a difference in the weight of two resistant lines, Col-0 and a transgenic *Rps2*^{KO} line with the Col-0 allele at insertion site two (*p* value > 0.45). Thus, neither the *rps2-101C* background and its associated truncated RPS2 protein, or the lox sites and nptII, impact plant performance directly or through an interaction with *Rps2*. Furthermore, both *Rps2*⁺ plant genotypes had significantly higher weight than both genotypes without *Rps2* (*p* value < 0.0005) when grown under sterile conditions. A comparison of *Rps2* isolines not created in the *rps2-101C* background

confirmed the growth benefit of *Rps2*: the Col-0 amiRNA knockdown line was significantly less fit than Col-0 (p value = 0.0026). Thus, removal of RPS2 protein is associated with reduced performance both in the *rps2*-101C and Col-0 backgrounds. In combination, these results demonstrate a beneficial pleiotropic function of *Rps2* measurable in stressful abiotic environments in the absence of pathogen.

***Rps2*-associated changes in defense response gene expression in the absence of pathogen**

To investigate novel functions of *Rps2* in the absence of pathogens, we determined the expression profile of two *Rps2^R*, one *Rps2^S*, and one *Rps2^{KO}* line grown in sterile conditions. We first contrasted the expression profiles of an *Rps2^R* and *Rps2^S* line that shared the same insertion site and exhibited similar expression levels. In the absence of pathogens, the difference between *R* and *S* alleles with similar expression levels was minimal (Supplementary Figure 5). The *Rps2^R* line had 14 genes that were upregulated and two genes that were downregulated relative to the *Rps2^S* line (Supplementary Figure 5). These genes were enriched for gene ontology (GO) annotations of response to stress, particularly for response to water stress (Supplementary Table 11; p value = 1.24E-05). The field fitness data displayed two patterns that we further explored with transcriptome data. First, we observed that *Rps2* knockout lines had lower lifetime fitness than *Rps2⁺* lines, essentially irrespective of *Rps2* expression level (Figure 2f). Second, given *Rps2* presence, there was an inverse relationship between *Rps2* expression level and fitness (Figure 2f). We explored the first of these two patterns, of *Rps2* presence or absence, by determining the expression profiles of three *Rps2⁺* lines and contrasting them with the *Rps2^{KO}* line. *Rps2⁺* lines upregulated 538 genes relative to *Rps2^{KO}* lines, and downregulated 312 genes. Genes upregulated in *Rps2⁺* plants were enriched for GO annotations involving photosynthesis and light response (Figure 3a; Supplementary Table 12; p values = 2.47E-03, 3.91E-05), while genes downregulated in *Rps2⁺* plants were enriched for stimulus response, stress response, biotic stimulus response, and defense response annotations (Figure 3b,c; Supplementary Table 13; p values = 1.18E-16, 3.57E-16, 7.41E-11, 9.01E-11). We found substantial overlap in genes differentially expressed in independent contrasts of single *Rps2⁺* lines and the *Rps2^{KO}* line (Figure 3d); genes identified in each single-line comparison were consistently enriched for the same GO annotations (Figure 3d; Supplementary Tables 14-19). Thus, removing both *R* and *S* alleles of *Rps2* from *A. thaliana* predominantly increased expression of genes that are induced in response to stress and pathogens.

We explored the second of these two patterns, *Rps2* expression level, by comparing the expression profiles of two Col-0 *Rps2^R* lines with high and low *Rps2* expression under sterile conditions. Expression of 36 genes was upregulated in the high *Rps2* expression line relative to the low *Rps2* expression line, and expression of 189 genes was downregulated (Figure 4a). Upregulated genes in the high *Rps2* expression line were enriched for genes involved in response to stimulus, particularly for thalianol metabolic processes (Figure 4a; Supplementary Table 20; p value = 1.05E-05). Downregulated genes in the high *Rps2* expression line were enriched for response to stimuli and stress, particularly for response to biotic stimulus and for the defense response (Figure 4a,b; Supplementary Table 21; p values = 3.38E-10, 1.75E-08, 1.67E-03, 4.03E-04). In contrast to the previous comparison between

Rps2⁺ and *Rps2*^{KO}, defense related genes were enriched in the downregulated gene set in the line with lower field fitness, or the line with higher *Rps2* expression level, rather than upregulated as in the *Rps2* knockout. The set of downregulated genes contained a subset that was differentially expressed in only the high *Rps2* expression line; this gene subset was also enriched for GO categories of response to stress and the defense response (Figure 4c; Supplementary Table 22; *p* values = 1.04E-02; 1.28E-02). *Rps2* overexpression therefore downregulated an additional, unique set of defense response genes than those induced in *Rps2* null mutants (Figure 4b,c). Thus, we observe enrichment for defense related genes that distinguish the highly fecund, low *Rps2* expression line from both the *Rps2* knockout and high *Rps2* expression lines, although the genes that contribute to these enrichments are different.

Discussion

Costs of resistance contribute to the long-term maintenance of polymorphism at defense genes because they help explain the persistence of susceptible alleles. However, it is hard to understand why the production of minute quantities of a recognition protein, such as those produced by *R*-gene loci, would entail a large physiological cost. It was therefore surprising that our emerging picture of the costs associated with *R*-gene loci is that they are large – on the order of 10%^{8,9}. Here, we report on the absence of a cost associated with *Rps2*, an *R*-gene that segregates for the maintenance of alternative alleles¹⁶. This result makes sense in that both *R* and *S* alleles are expressed in our *Rps2* isolines; thus, the difference between *R* and *S* genotypes is small relative to the difference in isolines segregating for indel polymorphisms, as in the previous *R*-genes for which costs have been measured^{8,9}. Since a large fraction of *R*-genes in the genome harbor multiple alleles^{29,30}, our results help explain how host genomes can tolerate the genetic load associated with *R*-gene resistance. We suggest that while stable indel polymorphisms may be maintained by large costs of resistance, stable non-indel *R*-gene polymorphisms are more likely to be maintained by a variety of ecological and physiological mechanisms, as elaborated below. Thus, this work reveals a fundamental effect of genetic architecture on the manifestation of costs of resistance.

Our creation of an artificial indel polymorphism for *Rps2* revealed a fitness benefit of up to 40% associated with the presence of *Rps2*, albeit an equivalent benefit for *R* and *S* alleles (Figure 2). The benefit of carrying an allele of *Rps2* appears to result from its function as a negative regulator of the defense response – loss of *Rps2* causes the upregulation of a number of genes involved in induced responses to stress (Figure 3; Supplementary Table 13). The critical function of *Rps2* provides a clear explanation for why *S* alleles are not deleted, as they typically are for *Rpm1* and *Rps5*; however, it does not explain the maintenance of both *R* and *S* alleles at *Rps2*. There are several possible explanations for the long-term maintenance of these clades. First, the *S* alleles may encode the ability to recognize effectors or pathogens that have yet to be identified, leading to selection for the retention of the functional “*S*” allele. Alternatively, the previously measured cost of attack⁷, in which the cost of response by *R* alleles of *Rps2* is a larger physiological burden than infection, may favor *S* alleles in certain environments. Such a benefit of susceptibility, even though environmentally restricted, could promote stable *Rps2* polymorphism⁴. Spatial or

temporal variation in other costs of resistance, namely in costs of surveillance or defense, could also promote stable *Rps2* polymorphism^{4,6}. Finally, spatial or temporal variation in costs of virulence in pathogens carrying *avrRpt2* could similarly promote stable polymorphism at *Rps2*^{4,31}.

More generally, functional *R*-gene alleles, when expressed, have the potential to carry a physiological cost due to expression or mis-expression^{20,21}. For *Rps2*, we observed a cost associated with increasing levels of expression (Figure 2f). Selection should act to minimize the costs associated with *R*-loci, especially costs of *S* alleles that have no pleiotropic, beneficial function. We suggest that a natural consequence of this selective process should be the deletion of *S* alleles, because deletions can carry no costs associated with their (mis)expression. Indeed, only when *S* alleles harbor beneficial effects should they be retained by selection, as is the case for *Rps2*. Our results thus demonstrate that defense loci segregating for functional alternatives, rather than for indel polymorphisms, limit the manifestation of costs of surveillance. Furthermore, our results suggest that genetic architecture both impacts, and is impacted by, physiological costs associated with segregating *R*-gene alleles. Given the substantial variation in *R*-gene evolutionary histories² and genetic architectures^{13,29,32}, it will be fascinating to further disentangle the complex interplay of genetic, physiological and ecological factors in the generation of diversity.

Methods

Cre-lox Insertion of RPS2

We introduced five intact alleles of *Rps2* into the same genomic location using a Cre-lox system in an *rps2-101C* mutant of Col-0³³, a plant line with a stop codon in RPS2 at amino acid 235 that is a presumed null mutation¹⁵ (Supplementary Figure 1). We also introduced an empty integration vector, without *Rps2*, to obtain empty vector insertions in the isogenic RPS2 null background (hereafter *Rps2*^{KO}). We repeated this process for each of three genomic locations, creating 18 isolines in all (Supplementary Table 1). Three alleles from the resistant clade, Col-0, Ct-0, and Ler-0 (*R* clade alleles or *Rps2*^R lines) were characterized as resistant in their native genetic background^{16,34}. One allele from the *R* clade, Ws-0 (*Rps2*^{pR}), was characterized as partially resistant in its native genetic background³⁴. One allele from the susceptible clade, Wu-0 (*S* clade allele or *Rps2*^S lines) was characterized as susceptible in its native genetic background¹⁴. The *Rps2*^R and *Rps2*^{pR} lines exhibited elevated HR and resistance compared to the *Rps2*^S and *Rps2*^{KO} lines upon infection with *P. syringae* pv. *avrRpt2*³⁵ (Supplementary Figures 6-7). Further details are included in the supplementary methods.

Field Fitness Experiment

Seedlings of each of 17 RPS2 lines were germinated in 98-cell trays containing 50:50 Metromix 200: Farfad C2 in the University of Chicago greenhouse. Plants with the Col-0 allele at insertion site one did not germinate. Seedlings were thinned on day seven of growth and flat locations were randomly cycled daily in the greenhouse to standardize growth conditions. On day 14, 100 seedlings per line were transplanted to a tilled field site in Downers Grove, Illinois, in a randomized block design in which each block contained a

plant from each *Rps2* line. Plants were set out in 15 rows of nine blocks, spaced by 0.25m within rows and by 1m between rows. Plants were irrigated for one week to reduce transplantation shock, and then sustained only by natural rainfall. The field was hand weeded once and plants received no other protection from competition or pests. 55% of plants died; the majority of these died in the first week presumably due to transplantation shock. Plant survival was evenly distributed among the allele types. Seven fitness proxies were measured: dry weight, undehisced seed set, seed size, silique number, average seeds per silique, and numbers of aerial and basal branches. Total seed set was estimated by multiplying silique number by the average number of seeds per silique.

Sampling for Pathogen Presence

96 plant samples representing all 17 lines were destructively harvested from the field on days 30 and 40 of growth. *P. syringae* was present in the majority of the plant samples, while *avrRpt2* was not seen in any sample. Sampling details are described in the supplementary methods.

Growth Chamber Fitness Experiment

1400 seedlings of seven lines with *Rps2* at insertion site two were germinated in 36-cell trays containing 25:25:50 Metromix 200:Farfad C2:Turfase in the University of Chicago growth chambers. Due to growth chamber size constraints, only lines from insertion site two were included. Seedlings were thinned and accessions were randomized within flats on day 7 of growth. After day 14, plants were watered every other day to mimic stressful growth conditions in the field. After six weeks of growth, we stopped watering and allowed the plants to dry for two weeks before processing. Two fitness proxies were measured: dry weight and undehisced seed set.

Sterile Plant Fitness Experiments

Two sets of lines were grown in sterile conditions. First, isogenic lines with *Rps2* at insertion site two were grown to measure fitness of plants with alleles of *Rps2* relative to the *Rps2* knockout. Second, four lines were measured to determine whether the truncated RPS2 protein present in the *rps2-101C* impacted the surveillance cost of *Rps2* resistance: Col-0, an amiRNA knockdown of RPS2 in a Col-0 background, and two lines on an isogenic *rps2-101CRps2* null background at insertion site two, one containing an insert of the Col-0 allele and one containing only the empty lox cassette. Further information on sterile conditions is included in the supplementary methods.

Fitness Analysis

R was used to specify nested linear models using the `lm` function from the stats package. Two sets of linear models were used to generate confidence intervals for each of seven fitness proxies at each insertion site for the field data, and for two fitness proxies for the growth chamber data. The field linear models included an effect of the date the plant was collected from the field. The growth chamber linear models included an effect of the date the plant was processed. The first set of models nested allele into either one of three (S, R, pR) or one of two (KO, *Rps2*⁺) allelic classes and considered each genomic insertion site

independently. The second set of models combined data for all genomic insertion sites to nest *Rps2* expression level into one of three allele classes (S, R, pR).

Quantitative real-time PCR

Expression of all *Rps2* isogenic lines was measured with qPCR using primers for *Rps2* and normalizing between samples using three reference genes: PP2A, Helicase, and bHLH³⁶. A subset of isogenic lines was used to compare *Rps2* expression in natural accessions to expression in the allelic series. Details of qPCR are described in the supplementary methods.

Whole Transcriptome Profiling

Plants with the Col-0 allele at insertion site two (R), the Col-0 allele at insertion site three (High R), the Wu-0 allele at insertion site two (S) or an empty vector at insertion site two (KO) were grown in sterile growth media as in the sterile plant fitness experiments. The Col-0 allele was chosen as the representative R allele for two reasons: 1) non-coding divergence was smallest between Col-0 and Wu-0 (Supplementary Figure 1b) and 2) *Rps2* gene expression variation existed to allow observation of expression level effects. Specific contrasts included: 1) R vs S; 2) R, 3) High R, and 4) S vs KO; and 5) High R vs R. RNA-seq and analysis followed standard protocols described in the supplementary methods.

Supplementary Material

Refer to Web version on PubMed Central for supplementary material.

Acknowledgements

We thank Heather King, Laura Merwin, Chris Meyer, Wayan Mulyati, Aaron Olsen, Nadia Shakoob, and Tom Stewart for their assistance in the field; Jean Greenberg for donation of strains for infection; Paul Hooykaas for pSDM3110, Madlen Vetter for her high-throughput infection protocol; and Ben Brachi, Talia Karasov, Martin Kreitman, and Laura Merwin for helpful discussions. This research was supported by NSF and NIH grants to J.B. and a grant from the National Natural Science Foundation of China to XQS (Grant no.: 31470448).

References

1. Tian D, Araki H, Stahl E, Bergelson J, Kreitman M. Signature of balancing selection in Arabidopsis. *Proc. Natl. Acad. Sci. U.S.A.* 2002; 99:11525–30. [PubMed: 12172007]
2. Bakker E, Toomajian C, Kreitman M, Bergelson J. A Genome-Wide Survey of R Gene Polymorphisms in Arabidopsis. *Plant Cell Online.* 2006; 18:1803–1818.
3. Thrall P, et al. Rapid genetic change underpins antagonistic coevolution in a natural host-pathogen metapopulation. *Ecol Lett.* 2012; 15:425–435. [PubMed: 22372578]
4. Brown J, Tellier A. Plant-Parasite Coevolution: Bridging the Gap between Genetics and Ecology. *Annu Rev Phytopathol.* 2011; 49:345–367. [PubMed: 21513455]
5. Brown JK. Durable resistance of crops to disease: a Darwinian perspective. *Annu Rev Phytopathol.* 2015; 53:513–39. [PubMed: 26077539]
6. Moreno-Gómez S, Stephan W, Tellier A. Effect of disease prevalence and spatial heterogeneity on polymorphism maintenance in host–parasite interactions. *Plant Pathol.* 2013; 62:133–141.
7. Korves T, Bergelson J. A novel cost of R gene resistance in the presence of disease. *Am. Nat.* 2004; 163:489–504. [PubMed: 15122498]
8. Tian D, Traw MB, Chen JQ, Kreitman M, Bergelson J. Fitness costs of R-gene-mediated resistance in Arabidopsis thaliana. *Nature.* 2003; 423:74–7. [PubMed: 12721627]

9. Karasov T, et al. The long-term maintenance of a resistance polymorphism through diffuse interactions. *Nature*. 2014; 512:436–440. [PubMed: 25043057]
10. Grant M, et al. Structure of the Arabidopsis RPM1 gene enabling dual specificity disease resistance. *Science*. 1995; 269(5225):843–846.
11. Stahl EA, Dwyer G, Mauricio R, Kreitman M, Bergelson J. Dynamics of disease resistance polymorphism at the Rpm1 locus of Arabidopsis. *Nature*. 1999; 400:667–71. [PubMed: 10458161]
12. Rose L, Atwell S, Grant M, Holub E. Parallel Loss-of-Function at the RPM1 Bacterial Resistance Locus in Arabidopsis thaliana. *Front Plant Sci*. 2012; 3:287. [PubMed: 23272006]
13. Meyers BC, Kozik A, Griego A, Kuang H, Michelmore RW. Genome-wide analysis of NBS-LRR-encoding genes in Arabidopsis. *Plant Cell*. 2003; 15:809–34. [PubMed: 12671079]
14. Kunkel B, Bent A, Dahlbeck D, Innes R, Staskawicz B. RPS2, an Arabidopsis Disease Resistance Locus Specifying Recognition of Pseudomonas syringae Strains Expressing the Avirulence Gene avrRpt2. *Plant Cell Online*. 1993; 5:865–875.
15. Yu GL, Katagiri F, Ausubel F. Arabidopsis mutations at the RPS2 locus result in loss of resistance to Pseudomonas syringae strains expressing the avirulence gene avrRpt2. *MPL*. 1993; 6(4):434–443. [PubMed: 8400373]
16. Mauricio R, et al. Natural selection for polymorphism in the disease resistance gene Rps2 of Arabidopsis thaliana. *Genetics*. 2003; 163:735–46. [PubMed: 12618410]
17. Out of 300 accessions with sequencing data (see supplemental methods), none have missing data or deletions called for Rps2.
18. Bergelson J, Purrington CB. Surveying patterns in the cost of resistance in plants. *American Naturalist*. 1996; 148(3):536–58.
19. Raj A, Rifkin S. Variability in gene expression underlies incomplete penetrance. *Nature*. 2010; 463
20. Mindrinos M, Katagiri F, Yu GL, Ausubel FM. The A. thaliana disease resistance gene RPS2 encodes a protein containing a nucleotide-binding site and leucine-rich repeats. *Cell*. 1994; 78:1089–99. [PubMed: 7923358]
21. Tao Y, Yuan F, Leister RT, Ausubel FM, Katagiri F. Mutational analysis of the Arabidopsis nucleotide binding site-leucine-rich repeat resistance gene RPS2. *Plant Cell*. 2000; 12:2541–2554. [PubMed: 11148296]
22. McNellis TW, Mudgett MB, Li K, Aoyama T. Glucocorticoid-inducible expression of a bacterial avirulence gene in transgenic Arabidopsis induces hypersensitive cell death. *The Plant Journal*. 1998; 14(2):247–257. doi:10.1046/j.1365-313X.1998.00106.x. [PubMed: 9628020]
23. Leister RT, Katagiri F. A resistance gene product of the nucleotide binding site -- leucine rich repeats class can form a complex with bacterial avirulence proteins in vivo. *The Plant Journal*. 2000; 22:345–54. [PubMed: 10849351]
24. Banerjee D, Zhang X, Bent A. The leucine-rich repeat domain can determine effective interaction between RPS2 and other host factors in Arabidopsis RPS2-mediated disease resistance. *Genetics*. 2001; 158:439–50. [PubMed: 11333251]
25. Axtell, McNellis, Mudgett, Hsu, Staskawicz. Mutational analysis of the Arabidopsis RPS2 disease resistance gene and the corresponding pseudomonas syringae avrRpt2 avirulence gene. *MPL*. 2001; 14:181–8. [PubMed: 11204781]
26. Day B, et al. Molecular Basis for the RIN4 Negative Regulation of RPS2 Disease Resistance. *Plant Cell Online*. 2005; 17:1292–1305.
27. Day B, Dahlbeck D, Staskawicz B. NDR1 Interaction with RIN4 Mediates the Differential Activation of Multiple Disease Resistance Pathways in Arabidopsis. *Plant Cell Online*. 2006; 18:2782–2791.
28. Qi D, DeYoung B, Innes R. Structure-function analysis of the coiled-coil and leucine-rich repeat domains of the RPS5 disease resistance protein. *Plant physiology*. 2012; 158:1819–32. [PubMed: 22331412]
29. Bergelson J, Kreitman M, Stahl EA, Tian D. Evolutionary dynamics of plant R-genes. *Science*. 2001; 292:2281–5. [PubMed: 11423651]
30. Gan X, et al. Multiple reference genomes and transcriptomes for Arabidopsis thaliana. *Nature*. 2011; 477:419–23. [PubMed: 21874022]

31. Laine AL, Tellier A. Heterogeneous selection promotes maintenance of polymorphism in host–parasite interactions. *Oikos*. 2008; 117:1281–1288. doi:10.1111/j.0030-1299.2008.16563.x.
32. Guo Y-LL, et al. Genome-wide comparison of nucleotide-binding site-leucine-rich repeat-encoding genes in *Arabidopsis*. *Plant Physiol*. 2011; 157:757–69. [PubMed: 21810963]
33. Vergunst AC, Jansen LE, Hooykaas PJ. Site-specific integration of *Agrobacterium* T-DNA in *Arabidopsis thaliana* mediated by Cre recombinase. *Nucleic Acids Res*. 1998; 26:2729–34. [PubMed: 9592161]
34. Caicedo AL, Schaal BA, Kunkel BN. Diversity and molecular evolution of the RPS2 resistance gene in *Arabidopsis thaliana*. *Proc. Natl. Acad. Sci. U.S.A.* 1999; 96:302–6. [PubMed: 9874813]
35. Guttman DS, Greenberg JT. Functional analysis of the type III effectors AvrRpt2 and AvrRpm1 of *Pseudomonas syringae* with the use of a single-copy genomic integration system. *Mol. Plant Microbe Interact*. 2001; 14:145–55. [PubMed: 11204777]
36. Czechowski T, Stitt M, Altmann T, Udvardi MK, Scheible W-RR. Genome-wide identification and testing of superior reference genes for transcript normalization in *Arabidopsis*. *Plant Physiol*. 2005; 139:5–17. [PubMed: 16166256]
37. Cao J, et al. Whole-genome sequencing of multiple *Arabidopsis thaliana* populations. *Nat. Genet*. 2011; 43:956–63. [PubMed: 21874002]

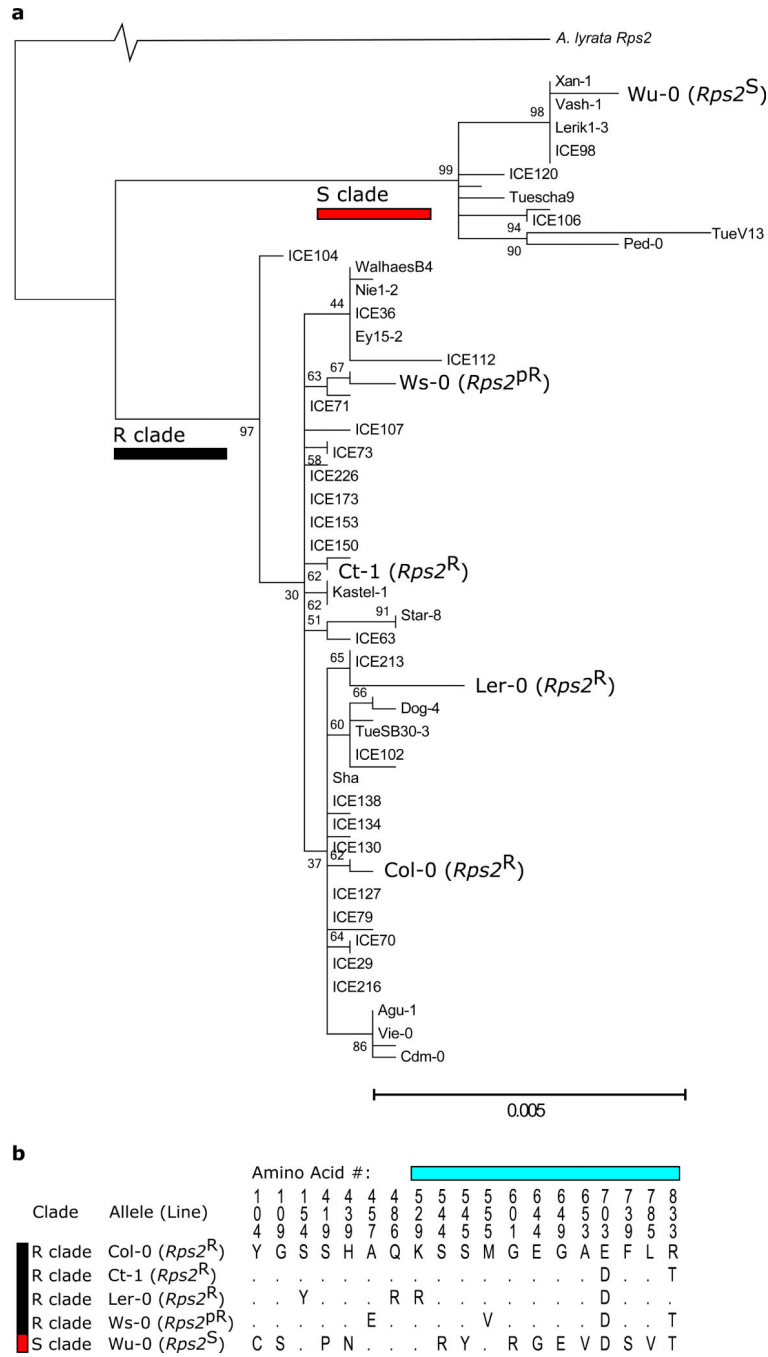


Figure 1. Natural variation in *Rps2* captured by the transgenic allelic series. Red and black bars indicate the susceptible and resistant clades of *Rps2* alleles, respectively. a) The two clades of *Rps2* alleles were inferred from the coding sequence of *Rps2* using maximum likelihood, and included 80 genomes from Cao *et al.*³⁷ and Sanger sequencing of the five alleles used in this study. The percentage of trees in which the associated taxa clustered together out of 1000 bootstrap replicates is shown next to the branches. b) Amino acid variation in the

alleles used in this study. Cyan bar indicates the Leucine-rich repeat region of *Rps2*; *Rps2^R* and *Rps2^{pR}* lines are resistant and partially resistant to *Pseudomonas syringae* pv. *avrRpt2*.

Author Manuscript

Author Manuscript

Author Manuscript

Author Manuscript

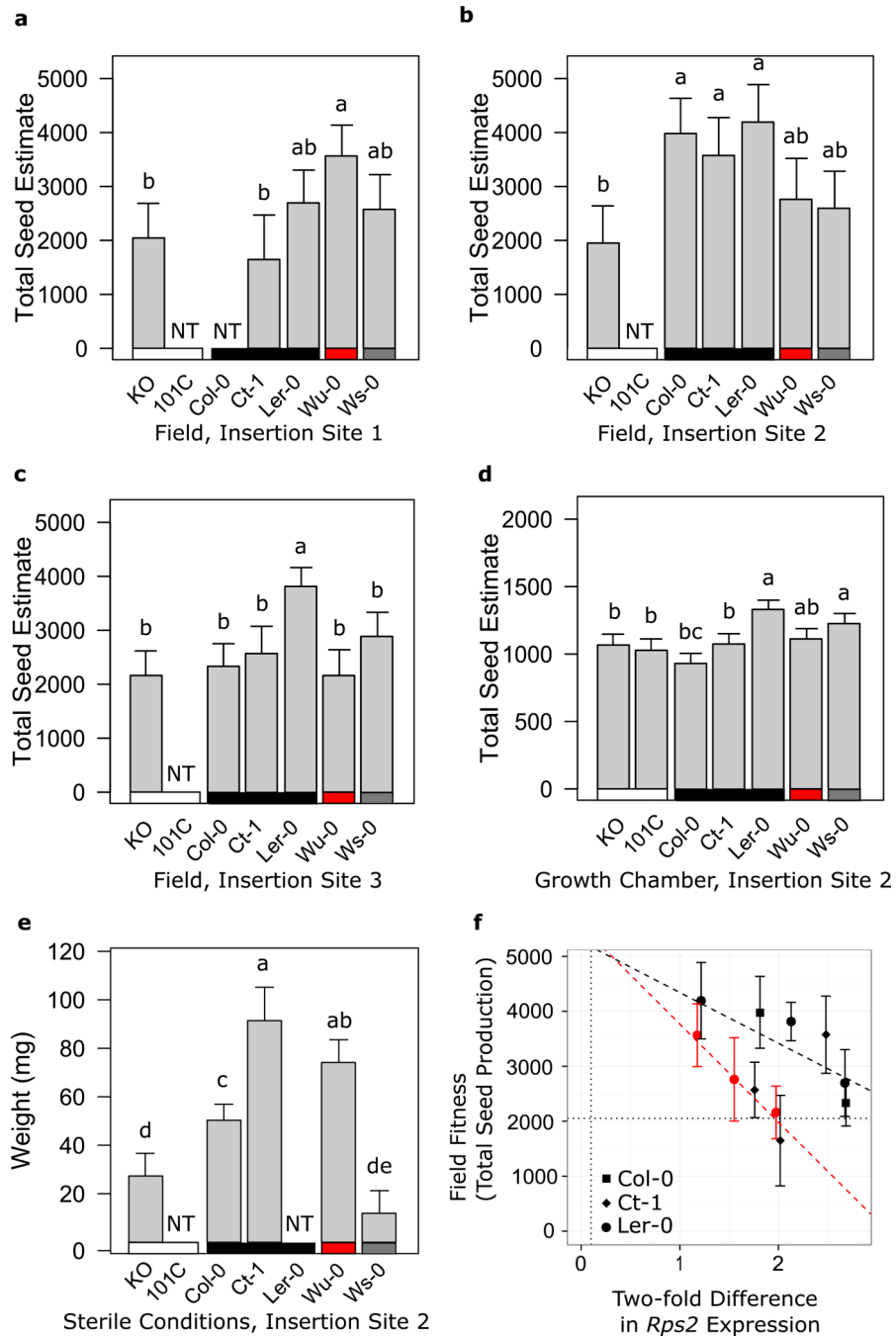


Figure 2. Significant fitness variation among lines in the allelic series in the absence of pathogen. KO is the *rps2*-101C mutant with empty lox sites at the insertion site for that line, referred to in the text as the *Rps2*^{KO} line; 101C is the *Rps2* null mutant without an inserted lox site. Lines with *Rps2* inserted at three genomic locations, or insertion sites, were tested. Black bar is under *Rps2*^R lines, grey bar is under *Rps2*^{PR} lines, red bar is under *Rps2*^S lines, and white bar is under *Rps2*^{KO} lines. Letters above bars within each insertion site indicate grouping using Tukey's post-hoc test. Lines with "NT" were not grown in this experiment. (a-c) Field

fitness results. a) Field fitness for insertion site one. The isoline with the Col-0 allele at insertion site one did not germinate. b) Field fitness for insertion site two. c) Field fitness for insertion site three. d) Growth chamber fitness for insertion site two. e) Sterile condition fitness for insertion site two. The isoline with the Ler-0 allele did not germinate in this experiment. f) Average *Rps2* expression at three weeks is negatively correlated with fitness in the field. The x-axis shows unitless relative expression of the isogenic lines (points) and the native accessions (vertical dotted line). Black and red dashed lines are the regression lines for the *R* and *S* clades, respectively, for the relationship between fitness and expression nested in allelic class. Black points are *Rps2^R* lines from the resistant clade of *Rps2*, and red points are *Rps2^S* lines from the susceptible clade of *Rps2*. The average fitness of the *Rps2* knockouts is plotted at the horizontal dotted line.

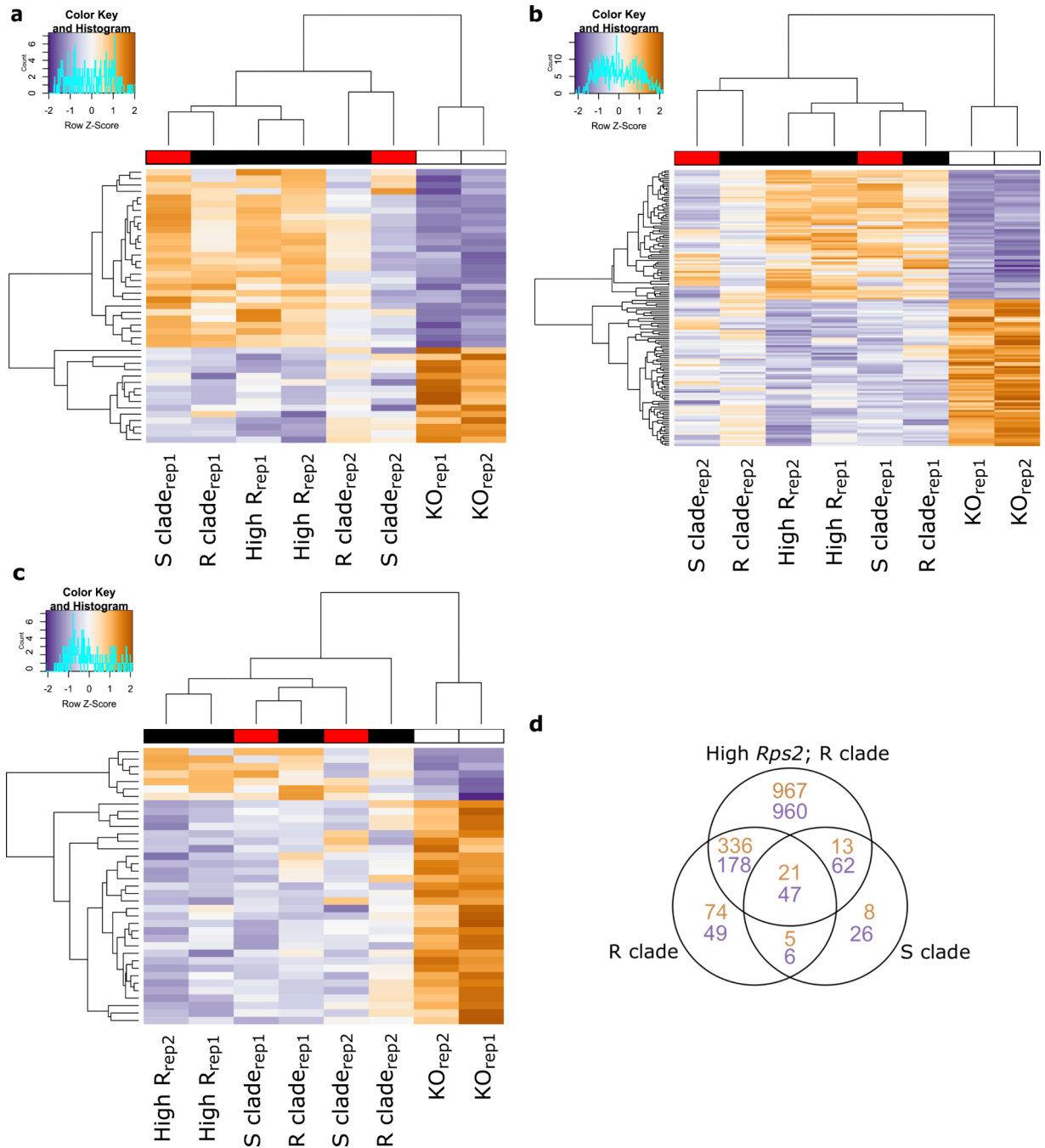


Figure 3. *Rps2* knockout lines differentially express stress response, defense response, and growth related genes relative to all lines with an allele of *Rps2*. R clade and S clade are resistant and susceptible *Rps2* lines, Col-0 and Wu-0, with similar levels of expression from insertion site two, and high R is the Col-0 allele of *Rps2* from insertion site three, which has a higher level of *Rps2* expression. (a-c) Heatmaps and dendrograms of gene sets as described below. Genes are in rows, and biological replicates are in columns, with both dendrograms grouped by similarity of expression in the gene set displayed. KO is the *rps2*-101C mutant with empty

lox sites at the insertion site two. a) Differentially expressed genes with GO annotations related to photosynthesis or response to light stimulus. b) Differentially expressed genes with GO annotations of response to stimulus or response to stress. c) Differentially expressed genes with GO annotations of defense response or response to biotic stimulus. d) The overlap of differentially expressed genes for three contrasts of lines with an *Rps2* allele and the knockout. Orange values are upregulated and blue are downregulated relative to the knockout.

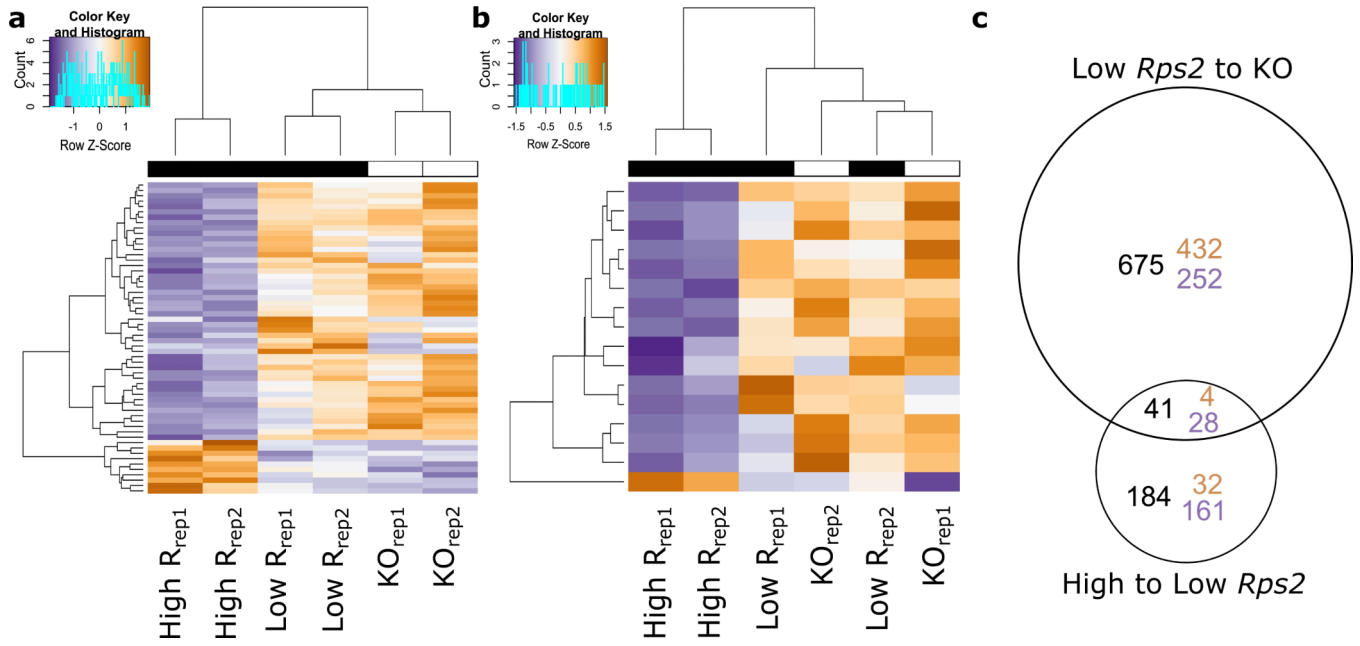


Figure 4. *Rps2* expression level affects both stress response and defense response genes. (a,b) Heatmaps and dendrograms of gene sets as described below. Genes are in rows, and biological replicates are in columns, with both dendrograms grouped by similarity of expression in the gene set displayed. KO is the *rps2-101C* mutant with empty lox sites at the insertion site two, low *R* is the Col-0 allele with a low level of expression from insertion site two, and high *R* is the Col-0 allele from insertion site three, which has a higher level of basal *Rps2* expression. a) Differentially expressed genes with GO annotations of response to stimulus or response to stress. b) Differentially expressed genes with GO annotations of defense response or response to biotic stimulus. c) The proportional overlap of genes differentially expressed between low and high *Rps2* expression lines with genes differentially expressed between the low expression line and the knockout. Orange values are upregulated and blue are downregulated relative to the knockout.